Angular surface solitons in sectorial hexagonal arrays

A. Szameit,[1,*] Y. V. Kartashov,[2] V. A. Vysloukh,[2] M. Heinrich,[1] F. Dreisow,[1] T. Pertsch,[1] S. Nolte,[1] A. Tünnermann,[1,3] F. Lederer,[4] and L. Torner[2]

[1]*Institute of Applied Physics, Friedrich-Schiller-University Jena, Max-Wien-Platz 1, 07743 Jena, Germany*
[2]*ICFO-Institut de Ciencies Fotoniques, and Universitat Politecnica de Catalunya, Mediterranean Technology Park, 08860 Castelldefels (Barcelona), Spain*
[3]*Fraunhofer Institute for Applied Optics and Precision Engineering, Albert-Einstein-Strasse 7, 07745 Jena, Germany*
[4]*Institute for Condensed Matter Theory and Optics, Friedrich-Schiller-University Jena, Max-Wien-Platz 1, 07743 Jena, Germany*
**Corresponding author: szameit@iap.uni-jena.de*

Received April 7, 2008; accepted April 24, 2008;
posted May 29, 2008 (Doc. ID 94737); published June 30, 2008

We report on the experimental observation of corner surface solitons localized at the edges joining planar interfaces of hexagonal waveguide array with uniform nonlinear medium. The face angle between these interfaces has a strong impact on the threshold of soliton excitation as well as on the light energy drift and diffraction spreading. © 2008 Optical Society of America

OCIS codes: 190.0190, 190.6135.

After the prediction of one-dimensional discrete surface solitons at the interface of uniform material and waveguide array with focusing nonlinearity [1] and at the interface between dissimilar arrays [2] and their subsequent observations [3–5], a burst of new findings revolutionized the perception of nonlinear surface waves. For example, solitons were found at the edge of defocusing lattices [6–8] and in two-dimensional (2D) geometries [2,9–11]. 2D surface solitons were observed in optically induced lattices [12] and in laser-written waveguide arrays [13–15]. However, up to now the impact of the geometry of the interface on the properties of 2D surface solitons was not addressed properly. To bridge this gap, we report in this Letter the salient features of 2D solitons localized at the edges joining planar interfaces of a focusing hexagonal waveguide array with a uniform nonlinear medium, and we show that the face angle is the key parameter defining the power threshold for soliton excitation and the direction of the light energy drift and diffraction spreading.

For the theoretical description of surface wave formation we employ the nonlinear Schrödinger equation for the dimensionless field amplitude q under the assumption of cw illumination:

$$i\frac{\partial q}{\partial \xi} = -\frac{1}{2}\left(\frac{\partial^2 q}{\partial \eta^2} + \frac{\partial^2 q}{\partial \zeta^2}\right) - q|q|^2 - pR(\eta,\zeta)q. \qquad (1)$$

Here η,ζ are the transverse coordinates and ξ is the longitudinal one; the parameter p characterizes the refractive index modulation depth; and the function $R(\eta,\zeta)$ describes refractive index profile in the array that can be represented as a superposition of Gaussian functions $\exp[-(\eta/w_\eta)^2-(\zeta/w_\zeta)^2]$. The waveguides with spacing d are arranged in a hexagonal structure where only those waveguides that are located within the face angle α between the planar interfaces are present. Thus, in a hexagonal structure the symmetry dictates five different types of interfaces (or corners) with angles $\alpha=n\pi/3$, where $n=1,\ldots,5$. We set $w_\eta=0.45$, $w_\zeta=0.9$, and $d=4$ in accordance with the transverse waveguide dimensions of 4.5 μm$\times$9 μm and the spacing of 40 μm. The parameter $p=2.8$ is equivalent to a refractive index change of 3.1×10^{-4}. In all cases we excite only the corner waveguides (see Fig. 1, showing a microscope image of hexagonal array and the excited waveguides).

The face angle α substantially affects the linear light propagation. The rate of discrete diffraction for a light beam launched in a corner waveguide increases with growing α and reaches its maximal value in the uniform hexagonal array. This is caused by the larger number of adjacent waveguides accompanying an increase of α, which results in a faster leakage of energy from the excited waveguide. Additionally, the light tends to drift from the excited corner waveguide into the array depth, but the rate of this process slows down with the growth of α. The integral center of the linear beam always shifts along the bisecting plane of the face angle α. Initially the transverse shift S of the integral beam center along

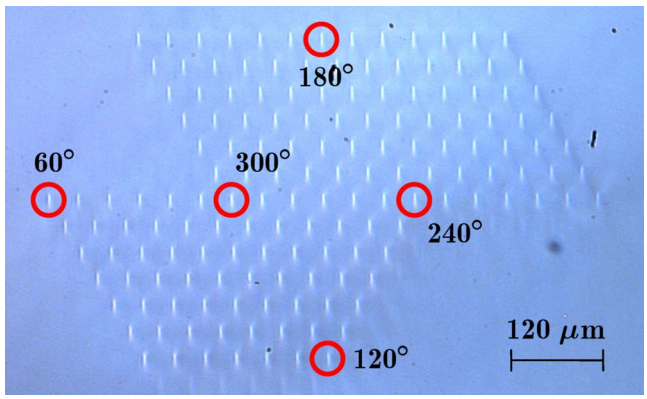

Fig. 1. (Color online) Microscope image of a laser written array. The excited waveguides are marked with a circle.

the bisecting line increases $\sim\xi^2$, but at larger distances one finds only a linear dependence $S\sim\xi$. For $\alpha=\pi/3$ and $2\pi/3$ the shift rate $dS/d\xi$ at larger distances is almost equal ($dS/d\xi=0.223$), but it drops to $dS/d\xi=0.168$ at $\alpha=\pi$ and to $dS/d\xi=0.031$ at $\alpha=5\pi/3$. Such a shift characterizes the diffraction anisotropy that appears owing to the specific boundary conditions.

The face angle α also strongly affects nonlinear excitations. Soliton solutions of Eq. (1) in the form $q=w(\eta,\zeta)\exp(ib\xi)$ can be characterized by the power $U=\int\int_{-\infty}^{\infty}w^2d\eta d\zeta$. For any α the corner solitons exist for b values above a cutoff b_{co} (Fig. 2) and for power above the threshold U_{th}, since the dependence $U(b)$ is nonmonotonic. In the region $b_{co}<b\leq b_{cr}$ one has $dU/db\leq 0$, which implies instability of the corresponding branch, while for $b>b_{cr}$ the solitons are stable, since $dU/db>0$. For $b\to b_{co}$ the solitons expand substantially across the waveguiding sector and acquire an asymmetric shape [Figs. 2(a) and 2(c)], while far from cutoff the light localizes in the corner waveguide [Fig. 2(b)]. At $b\to\infty$, when the soliton becomes very narrow and the lattice role diminishes, the power approaches that of Townes soliton, i.e., $U=5.85$. The threshold power of corner solitons increases with increase of the face angle α, since for higher α the nonlinearity has to counterbalance the stronger discrete diffraction. Hence, the threshold power varies notably from $U_{th}=0.622$ for $\alpha=\pi/3$ to $U_{th}=0.741$ for $\alpha=\pi$ and $U_{th}=0.809$ for $\alpha=5\pi/3$.

This trend is clearly seen in experiments performed in a waveguide array written with femtosecond laser pulses (Coherent Mira/RegA; see [16] for details of fabrication). The topology of this array (Fig. 1) allowed us to include all five types of wedge-like interfaces (from $\alpha=\pi/3$ to $\alpha=5\pi/3$ in a single structure. The writing velocity was 2000 μm/s, which ensures a nonlinear coefficient similar to that in the bulk material [17]. The spacing $d=40$ μm yields almost isotropic coupling between adjacent waveguides [13]. The length of the sample was 105 mm, and the transmission losses of a single waveguide were <0.4 dB/cm. For soliton excitation we used a Ti:sapphire chirped-pulse-amplification laser system (Spitfire, Spectra-Physics) with a pulse duration of 150 fs and a repetition rate of 1 kHz at 800 nm. In Fig. 3 the observed light evolution in the wedge-like array with $\alpha=\pi/3$ is shown and compared with the simulations according to Eq. (1). The experimental images taken upon excitation of different waveguides were rotated in order to have the face angle increasing counterclockwise for different arrays. Owing to the small face angle between the interfaces, the light penetrates notably into the array depth and the displacement of the integral beam center is rather strong at small power levels [Fig. 3(a)]. With increasing power, the output intensity distribution contracts toward the corner waveguide [Fig. 3(b)], so that at sufficiently high powers the drift and diffraction spreading are suppressed and a discrete corner soliton forms [Fig. 3(c)]. Since in this specific case ($\alpha=\pi/3$) the excited waveguides has only three neighbors, the power of the input beam required for soliton formation is smaller than in other configurations, even though the displacement of the integral center is maximal. This becomes apparent when the light evolution is compared with that in an array with a straight planar interface ($\alpha=\pi$), which is shown in Fig. 4. In the linear case, the light again spreads deeply into the array region. However, the displacement of the integral beam center is substantially smaller than in the wedge-like geometry [Fig. 4(a)]. For an increasing input peak power the beam center at the output again moves toward the excited waveguide [Fig. 4(b)]. If the launched beam power exceeds a certain threshold, a discrete surface soliton forms [Fig. 4(c)]. However, the power threshold for $\alpha=\pi$ is considerably higher than for $\alpha=\pi/3$ owing to an in-

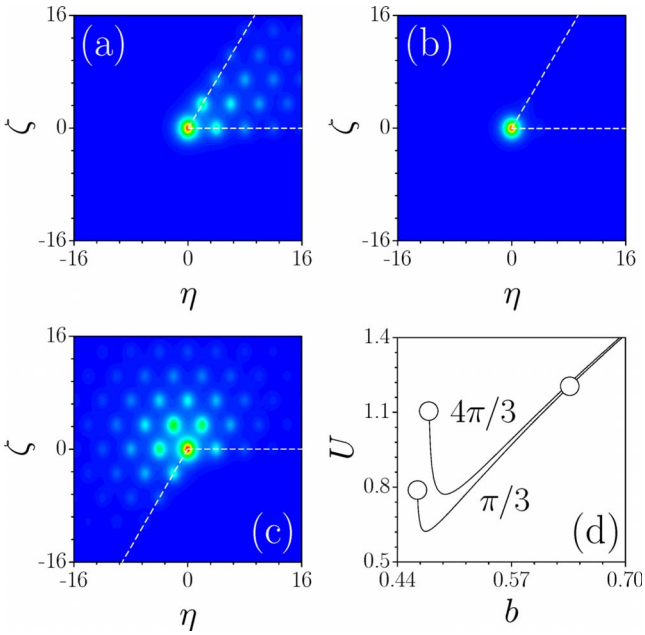

Fig. 2. (Color online) Profiles of surface solitons at (a) $b=0.463$, $\alpha=\pi/3$; (b) $b=0.637$, $\alpha=\pi/3$; and (c) $b=0.476$, $\alpha=4\pi/3$, corresponding to the points marked with circles in the (d) $U(b)$ diagrams. The white dashed lines indicate the interface position. In all cases $p=2.8$.

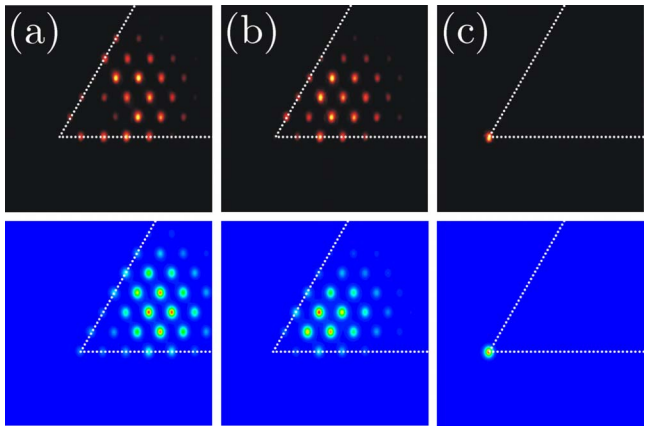

Fig. 3. (Color online) Comparison of the output intensity distributions for an excitation of a corner waveguide in an array with $\alpha=\pi/3$. Top row, experiment; bottom row, theory. The input power is (a) 0.15 MW, (b) 1.3 MW, and (c) 3.2 MW.

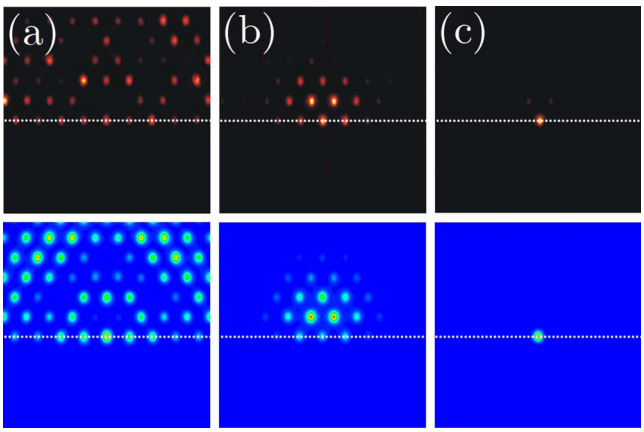

Fig. 4. (Color online) Comparison of the output intensity distributions for an excitation of a corner waveguide in an array with $\alpha=\pi$. Top row, experiment; bottom row, theory. The input power is (a) 0.15 MW, (b) 2.5 MW, and (c) 3.5 MW.

creased number of neighboring waveguides and the stronger discrete diffraction.

A sequence of output intensity distributions for increasing input peak powers in a concave geometry ($\alpha=4\pi/3$) is depicted in Fig. 5. In the low power limit the light spreads into the array region, while the integral beam center is only slightly shifted from the excited waveguide [Fig. 5(a)]. With increasing input peak power, the diffraction spreading is suppressed [Figs. 5(b) and 5(c)]. For sufficiently high input peak powers one can clearly observe near-corner localization [Figs. 5(d) and 5(e)], and finally a corner soliton forms [Fig. 5(f)]. The required threshold power is again larger than in the previous cases, since now there are five neighbors of the excited guide yielding a further enhanced diffraction.

In conclusion, we demonstrated experimentally 2D solitons at the edges joining planar interfaces of a hexagonal waveguide array with a uniform nonlinear medium. In the linear limit the displacement of the integral beam center is maximal for small face angles α, and it decreases with growing α. In contrast, the threshold power for soliton formation substantially increases with an increase of α.

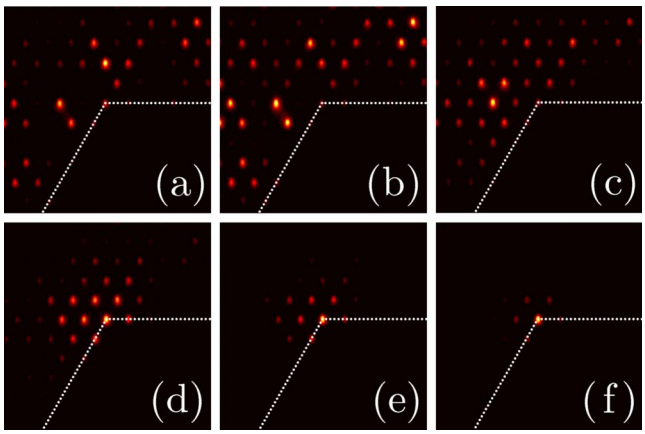

Fig. 5. (Color online) Dynamic excitation of a corner waveguide in an array with $\alpha=4\pi/3$. The input power is (a) 0.15 MW, (b) 1 MW, (c) 2 MW, (d) 2.3 MW, (e) 2.7 MW, and (f) 3.7 MW.

The authors wish to thank the Deutsche Forschungsgemeinschaft (Research Group "Nonlinear spatial-temporal dynamics in dissipative and discrete optical systems" FG 532). This work has also been supported by the Government of Spain through the Ramon-y-Cajal program and through grant TEC2005–07815.

References

1. K. G. Makris, S. Suntsov, D. N. Christodoulides, G. I. Stegeman, and A. Haché, Opt. Lett. **30**, 2466 (2005).
2. K. G. Makris, J. Hudock, D. N. Christodoulides, G. I. Stegeman, O. Manela, and M. Segev, Opt. Lett. **31**, 2774 (2006).
3. S. Suntsov, K. G. Makris, D. N. Christodoulides, G. I. Stegeman, A. Haché, R. Morandotti, H. Yang, G. Salamo, and M. Sorel, Phys. Rev. Lett. **96**, 063901 (2006).
4. S. Suntsov, K. G. Makris, D. N. Christodoulides, G. I. Stegeman, R. Morandotti, M. Volatier, V. Aimez, R. Arès, C. E. Rüter, and D. Kip, Opt. Express **15**, 4663 (2007).
5. S. Suntsov, K. G. Makris, D. N. Christodoulides, G. I. Stegeman, R. Morandotti, H. Yang, G. Salamo, and M. Sorel, Opt. Lett. **32**, 3098 (2007).
6. Y. V. Kartashov, V. A. Vysloukh, and L. Torner, Phys. Rev. Lett. **96**, 073901 (2006).
7. C. R. Rosberg, D. N. Neshev, W. Krolikowski, A. Mitchell, R. A. Vicencio, M. I. Molina, and Y. S. Kivshar, Phys. Rev. Lett. **97**, 083901 (2006).
8. E. Smirnov, M. Stepic, C. E. Rüter, D. Kip, and V. Shandarov, Opt. Lett. **31**, 2338 (2006).
9. Y. V. Kartashov, V. A. Vysloukh, D. Mihalache, and L. Torner, Opt. Lett. **31**, 2329 (2006).
10. R. A. Vicencio, S. Flach, M. I. Molina, and Y. S. Kivshar, Phys. Lett. A **364**, 274 (2007).
11. H. Susanto, P. G. Kevrekidis, B. A. Malomed, R. Carretero-Gonzalez, and D. J. Frantzeskakis, Phys. Rev. E **75**, 056605 (2007).
12. X. Wang, A. Bezryadina, Z. Chen, K. G. Makris, D. N. Christodoulides, and G. I. Stegeman, Phys. Rev. Lett. **98**, 123903 (2007).
13. A. Szameit, Y. V. Kartashov, F. Dreisow, T. Pertsch, S. Nolte, A. Tünnermann, and L. Torner, Phys. Rev. Lett. **98**, 173903 (2007).
14. A. Szameit, Y. V. Kartashov, F. Dreisow, M. Heinrich, V. Vysloukh, T. Pertsch, S. Nolte, A. Tünnermann, F. Lederer, and L. Torner, Opt. Lett. **33**, 663 (2008).
15. A. Szameit, Y. V. Kartashov, F. Dreisow, M. Heinrich, T. Pertsch, S. Nolte, V. Vysloukh, A. Tünnermann, and L. Torner, Opt. Lett. **33**, 1132 (2008).
16. A. Szameit, J. Burghoff, T. Pertsch, S. Nolte, and A. Tünnermann, Opt. Express **14**, 6055 (2006).
17. D. Blömer, A. Szameit, F. Dreisow, T. Schreiber, S. Nolte, and A. Tünnermann, Opt. Express **14**, 2151 (2006).